J Mater Sci: Mater Med (2010) 21:1233–1239
DOI 10.1007/s10856-010-3989-5

The release of nickel from nickel–titanium (NiTi) is strongly reduced by a sub-micrometer thin layer of calcium phosphate deposited by rf-magnetron sputtering

R. A. Surmenev · M. A. Ryabtseva · E. V. Shesterikov · V. F. Pichugin · T. Peitsch · M. Epple

Received: 25 August 2008 / Accepted: 4 January 2010 / Published online: 30 January 2010

Abstract Thin calcium phosphate coatings were deposited on NiTi substrates (plates) by rf-magnetron sputtering. The release of nickel upon immersion in water or in saline solution (0.9% NaCl in water) was measured by atomic absorption spectroscopy (AAS) for 42 days. The coating was analyzed before and after immersion by X-ray powder diffraction (XRD), scanning electron microscopy (SEM) and energy-dispersive X-ray spectroscopy (EDX). After an initial burst during the first 7 days that was observed for all samples, the rate of nickel release decreased 0.4–0.5 ng cm^{-2} d^{-1} for a 0.5 μm-thick calcium phosphate coating (deposited at 290 W). This was much less than the release from uncoated NiTi (3.4–4.4 ng cm^{-2} d^{-1}). Notably, the nickel release rate was not significantly different in pure water and in aqueous saline solution.

1 Introduction

Nickel–titanium (NiTi) finds application in clinical medicine due its special mechanical properties, i.e. the shape-memory effect and the superelasticity [1]. Typical examples are orthodontic wires [2], stents [3], porous intervertebral disks [4], and clamps for foot surgery [5, 6]. However, it is known that nickel ions are potentially allergenic, carcinogenic, teratogenic, and genotoxic [7, 8] and concerns have been raised regarding a release of nickel from NiTi implants [4, 9–11]. Although the amount of released nickel from NiTi is typically of the order of some tens of ng cm^{-2} d^{-1} only (see Ref. [12] for a literature survey), the issue of nickel release is still under discussion in the case of biomedical materials [4, 11]. The reported amount of released nickel is far lower than the standard dietary intake of Ni (150–900 μg per day [13]), but for a biomedical application, an enrichment of locally released nickel in the vicinity of an implant may still be decisive.

In any case, it would be beneficial for nickel-containing biomaterials to constrain nickel to the bulk of the metal and thereby to prevent its leaching into the surrounding tissue [11]. Experiments on the release of nickel were carried out by many authors, e.g. on nickel-containing stainless steel [14, 15], NiTi [10–12, 16, 17], Cu18Ni20Zn [18], 83Cu2Ni10Zn5Sn, 62.5Cu23Ni12Zn2.5Sn, and 32Cu66Ni2Fe [19]. Many studies on the release of nickel from NiTi are discussed in Refs. [4, 11, 12]. The rate of nickel release strongly depends on the experimental conditions, the immersion media and also on the surface treatment of the NiTi phase. Shabalovskaya et al. have recently discussed the delicate interplay between a NiTi surface treatment and the possible release of nickel, and made a strong point that the nature of the surface of the material under investigation must be clearly studied in order to interpret the release of nickel [11]. Bansiddhi et al. have recently reviewed the release of nickel from porous NiTi implants [4].

Different treatments for NiTi were developed to decrease the release of nickel from nickel-containing alloys, e.g. mechanical and electrochemical treatments, chemical etching, heat treatments, conventional and laser and electron beam irradiation [11], plasma immersion ion implantation

R. A. Surmenev (✉) · M. A. Ryabtseva · E. V. Shesterikov · V. F. Pichugin
Department of Theoretical and Experimental Physics, Tomsk Polytechnic University, 634050 Tomsk, Russia
e-mail: surmenev@tpu.ru

T. Peitsch · M. Epple
Inorganic Chemistry and Center for Nanointegration Duisburg-Essen (CeNIDE), University of Duisburg-Essen, 45117 Essen, Germany

(PIII) both in oxygen or nitrogen atmosphere to create a thin oxide or nitride layer that increases the corrosion resistance of the surface [4, 12, 16, 17, 20], carbon plasma immersion ion implantation [21], and immersion into Hank's buffer (HBS) to form a calcium phosphate layer [22]. Calcium phosphate is beneficial for materials in hard tissue contact because it is highly biocompatible [23].

There is little information in the literature about experiments on the release of nickel from NiTi coated with calcium phosphate. To enhance the bioactivity and also to decrease the nickel release, Jiang and Rong prepared crystalline hydroxyapatite ($Ca_5(PO_4)_3OH$) layers on porous NiTi by chemical treatment (32.5% HNO_3 solution followed by boiling in 1.2 M NaOH solution) and subsequent immersion into *simulated body fluid* (SBF) for five days [24]. The resulting hydroxyapatite layer uniformly covered the porous NiTi, both on the surfaces and within the pores. The release of nickel was even lower than in untreated dense NiTi (up to 50 days). The total amount of nickel released from a porous NiTi alloy with hydroxyapatite coating was 7.2 μg after 1200 h immersion in (SBF). In comparison, about 100 μg were released from an untreated NiTi sample [24]. There were also some attempts to coat NiTi with calcium phosphate by the dipping it into supersaturated calcium phosphate solution (SCS) [25–27]. However, it was shown later that the etching necessary for surface activation leads to an increased release of nickel from the surface layer [11].

A physically-deposited thin biocompatible coating which also acts as barrier for nickel ions should be well suited to decrease the nickel release rate, and it would also improve the surface properties in contact with hard tissue like bone. Such a coating must meet some requirements which are dictated by its subsequent clinical use, i.e. thickness, chemical composition and adhesion strength. Rf-magnetron sputtering allows the deposition of thin, dense and pore-free calcium phosphate coatings with high adhesion strength to different metallic substrates such as Ti6Al4V [28, 29], NiTi [30] and titanium [30]. It does not require a chemical treatment for activation of the NiTi surface which is necessary for coating by immersion into supersaturated calcium phosphate solutions. In comparison to standard methods to passivate the surface of NiTi by oxidation or nitridation, it leads to a more bioactive coating of calcium phosphate which will be advantageous in bone contact. It was recently shown that a thin calcium phosphate coating can be prepared by rf-magnetron sputtering using a hydroxyapatite target, and that its adhesion strength is very high for a thickness below 1.6 μm [30].

Here a proof-of-concept for this coating procedure is reported, i.e. on the time-resolved measurement of the nickel release from calcium phosphate-coated NiTi surfaces in both pure water and 0.9% aqueous NaCl solution.

2 Materials and methods

Nickel titanium alloy (NiTi) (superelastic, "medical grade") obtained from Memory Metalle GmbH, Germany, with $A_p = 21.5°C$ (preceded by an endothermal peak at 0.2°C) and $M_p = 16.4°C$ was used as substrate. A NiTi plate ($200 \times 200 \times 0.2$ mm^3 = width × length × thickness) was cut into pieces of $10 \times 10 \times 0.2$ mm^3 by shear pressing (a cold metal-cutting method). Thus, the samples were not subjected to heat during the cutting and the surface properties were probably not affected. The surface area of each sample was 2.08 cm^2. Before the deposition procedure, all samples were cleaned by boiling in carbon tetrachloride (CCl_4), followed by drying in gaseous nitrogen/isopropyl alcohol and washing in distilled water. The surface roughness corresponded to class 8 ($R_a = 0.56 \pm 0.03$ μm).

A commercially available installation 08PKHO-100T-005 for plasma etching with a custom-made rf-magnetron source (5.28 MHz) was used to deposit the calcium phosphate coatings. Thin calcium phosphate coatings with up to 0.6 μm thickness were deposited at a pressure of 0.1 Pa in either oxygen or argon atmosphere for 2 h. The whole surface of the samples was covered with calcium phosphate by 2 deposition runs, i.e. one side was coated and then the sample was turned and the other side was coated. By this procedure, the edges of the sample were partially covered with calcium phosphate. The sample surface temperature during deposition was measured with a chromel-copel thermocouple.

For scanning electron microscopy, an ESEM Quanta 400 FEG instrument from FEI, equipped with energy-dispersive X-ray analysis (EDX; EDS analysis system Genesis 4000, SUTW-Si(Li) detector), operating in high vacuum, was used. The samples were sputtered with gold/palladium before the SEM study. The EDX spectra were collected for 60 s with a dead time of 30%, the distance between the samples and the source of electrons was set to 10 mm, and the energy of the analyzing electron beam was 10 keV. Thickness and roughness of the coating were determined with a mechanical profilometer Talysurf 5 (Tyler-Hobson, England). The coating thickness was determined by shielding a part of each sample from the deposition process, thereby preventing the coating formation on this part of the sample. The thickness of the coatings was then calculated by measuring the profile of the resulting edge and determination of the step height. The profilometer vertical resolution was 10 nm and the horizontal resolution was 2 μm (given by the radius of the scanning needle). In addition, the coating thickness was measured by embedding the sample, cutting and grinding and direct observation in the SEM. X-ray powder diffraction (XRD) was carried out with a Shimadzu XRD-6000 diffractometer operating with Cu K_α radiation

($\lambda = 1.5406$ Å) at 40 kV and 30 mA in Bragg–Brentano mode. As references, synthetic hydroxyapatite (#9-0432) and nickel titanium (cubic austenite phase) (#18-0899) from the ICDD database were used.

Nickel release experiments were carried out both in pure water (Pure-lab Ultra Instrument from ELGA) and in 0.9% NaCl saline solution. Ultrapure NaCl was obtained from Merck (Suprapur®; max. 0.01 ppm Ni in solid NaCl according to the manufacturer; no detectable nickel by AAS in 0.9% aqueous solution). The concentration of nickel in all media before the experiments was below the instrumental detection limit (0.2 ppb). The samples were completely immersed either into water or into 0.9 wt% NaCl solution for 42 days at 37°C (60 ml in both cases). The sample volume was 0.02 cm^3, i.e. the volume ratio of water to NiTi was 3000:1. The solution was not stirred. After selected time intervals (2 d, 7 d, 14 d, 28 d, 35 d, and 42 d), 1 ml of the solution was removed and used to determine the nickel concentration. This volume was not replaced to avoid contamination. The amount of released nickel per sample surface (accumulated mass of released nickel, μg cm^{-2}) was computed as

$$m_{Ni} = V_p \cdot C_{Ni}/S_{surf}. \quad (1)$$

with V_p the total solution volume (starting with 60 ml, then 59 ml, 58 ml, etc.), C_{Ni} the concentration of nickel in ppb (μg l^{-1}), S_{surf} the sample surface area (2.08 cm^2) and m_{Ni} the cumulated nickel release rate (μg cm^{-2}). Each release experiment was carried out with four identical samples, and the results were averaged after the experiment.

The nickel release was measured by atomic absorption spectroscopy (AAS). An AA Spectrometer M Series with a GF 95 graphite furnace autosampler was used (detection limit: 0.2 ppb). For each sample, two determinations of the released nickel at the same time interval were carried out.

3 Results and discussion

The deposition parameters used are summarized in Table 1.

In Fig. 1, typical X-ray diffraction patterns of calcium phosphate coatings deposited at 30 and 290 W are shown.

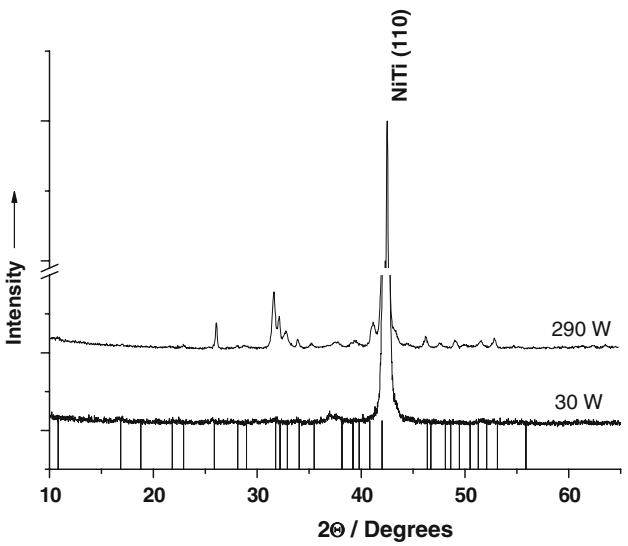

Fig. 1 X-ray diffraction patterns of calcium phosphate coatings deposited at 30 and 290 W in argon atmosphere. The coating deposited at 290 W is much more crystalline than that deposited at 30 W. The vertical lines show the computed peak positions for hydroxyapatite

Due to the thin coatings, the underlying NiTi substrate also gives diffraction peaks in both cases. The calcium phosphate coating deposited at 30 W was X-ray amorphous whereas the coating deposited at 290 W consisted of nanocrystalline hydroxyapatite. This difference may be explained by the higher substrate temperature at 290 W which induced the crystallization process, facilitated by higher adatom mobility on the surface. At low rf-power it is not possible for an adatom arriving at the substrate surface to gain enough energy to diffuse on the surface and to induce crystallization, therefore all ions and atoms are stuck on the surface and form an amorphous coating. A significant difference between argon and oxygen atmospheres for both powers was not observed. The hydroxyapatite peaks (211), (112), (300), and (002) were indexed for the coatings deposited at an rf-power of 290 W at 31.7°, 32.1°, 32.9° and 25.9°, respectively. With the program Powder Cell 2.4 (PCDWIN), a full-profile analysis program that takes into account the angle-dependent peak diffraction broadening, the size of the average coherent-scattering regions (CSR)

Table 1 Deposition parameters for the calcium phosphate coatings by rf-magnetron sputtering

rf-power (W)	Working atmosphere	Sample surface temperature (°C)	Coating thickness (μm)
290	Ar	300	0.6 ± 0.1
290	O_2	300	0.5 ± 0.1
30	Ar	130	0.1 ± 0.02
30	O_2	130	0.1 ± 0.02

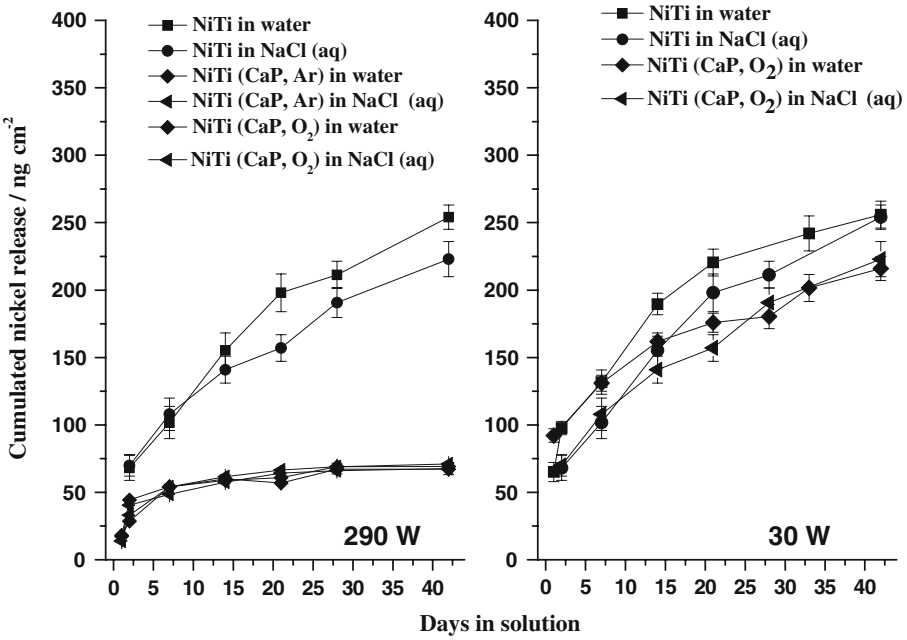

Fig. 2 Cumulated nickel release measured for coatings deposited at 290 and 30 W, both in argon and in oxygen atmosphere. The samples were immersed either in water or in aqueous saline solution. For comparison, the nickel release from uncoated NiTi samples was also measured. Four samples were measured for each datapoint, and the standard deviation is given as error bars

was computed to 50 ± 10 nm and the averaged internal elastic stress to $\Delta d/d = (7 \pm 1) \cdot 10^{-3}$. The stress within the coating probably results from the deposition process.

In the Fig. 2, the cumulated values for the nickel release during 42 days immersion are shown, and the numerical data are summarized in Table 2. There was an initial burst for all samples during the first 7 days. This was probably due a release of nickel from the surface layer of each sample before passivation occurred by formation of TiO_2 [11]. After that initial period, the rate of nickel release decreased to 0.4–0.5 ng cm^{-2} d^{-1} for samples coated at 290 W. No influence of the working atmosphere (Ar or O_2) was found. The slightly lower release of nickel in NaCl solution as compared to pure water is not considered to be statistically significant. In contrast, there was an almost constant ongoing release for both uncoated NiTi and NiTi coated at 30 W. These values were 7–10 times higher compared to NiTi samples coated at 290 W. A microscopic investigation of the coating that was deposited at 30 W showed that it had either completely dissolved or was completely delaminated after 42 days of exposure (Fig. 3). An additional parallel experiment showed that the coating deposited at 30 W had completely vanished after 24 h immersion into water or saline solution. This could be either due to a high solubility of the amorphous coating or due to a poor adhesion to the substrate. At present, it cannot be distinguished between these two possibilities. Again, no influence of the working atmosphere (Ar or O_2) was found for the coatings deposited at 30 W.

Figure 3 shows the surface morphology of the coating and its elemental composition before and after the immersion. The typical relief structure of the original NiTi was not changed by the coating procedure (Fig. 3a), i.e. the thin coating followed the surface morphology of underlying NiTi substrate. EDX clearly shows the calcium phosphate layer (Fig. 3b). After 42 days of immersion in saline solution (identical results were obtained for immersion in water), the coating had partially delaminated (Fig. 3c), and both calcium and phosphate were partially dissolved (Fig. 3d). In contrast, the thin coatings deposited at 30 W

Table 2 The average nickel release rate calculated for water and saline solutions

Sample	Average nickel release rate (ng cm^{-2} d^{-1})			
	Pure water		Aqueous saline solution (0.9% NaCl)	
	Days 0–7	Days 7–42	Days 0–7	Days 7–42
CaP (290 W, O_2 and Ar)	7.7 ± 0.1	0.4 ± 0.1	6.9 ± 0.1	0.5 ± 0.1
CaP (30 W, O_2)	18.8 ± 1.3	3.6 ± 0.3	18.7 ± 0.9	2.4 ± 0.3
Uncoated NiTi	14.5 ± 1.7	4.4 ± 0.3	15.3 ± 1.7	3.4 ± 0.4

No difference was observed between sputtering in argon or oxygen. The average release rates were computed as $[c(\mathrm{Ni}, t_1) - c(\mathrm{Ni}, t_0)]/(t_1 - t_0)$

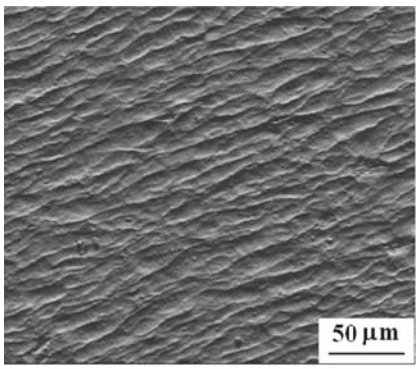

(a) 290 W before immersion

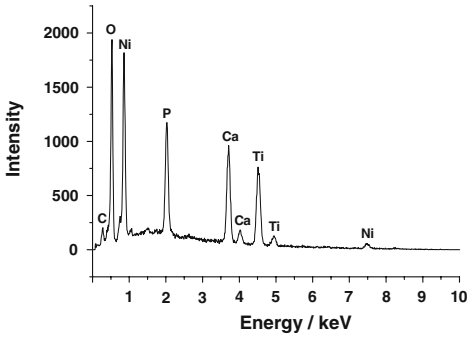

(b) Ca/P=1.67 to 1.75

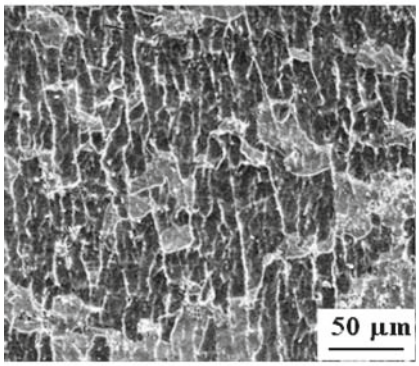

(c) 290 W after immersion

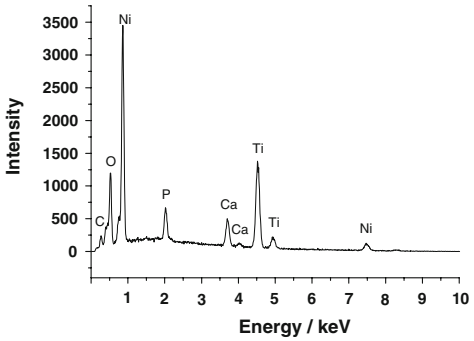

(d) Ca/P=1.56 to 1.65

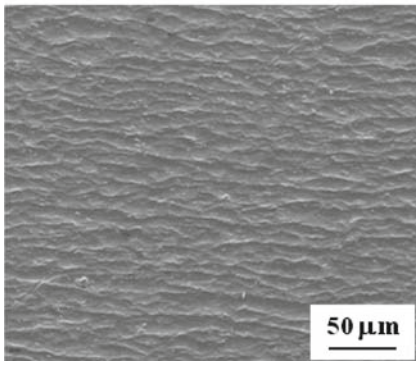

(e) 30 W after immersion

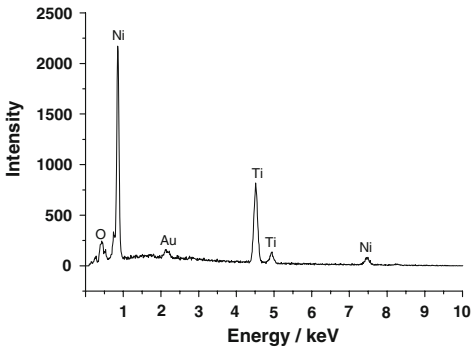

(f) no detectable calcium or phosphorus

Fig. 3 Scanning electron micrographs and EDX–spectra of the as-deposited coating deposited at 290 W (**a**, **b**), of the coating deposited at 290 W after 42 days of immersion in saline solution (**c**, **d**), and of the coating deposited at 30 W after 42 days of exposure in saline solution (**e**, **f**). The peak from Au at 2.12 keV in Fig. 3f is due to gold sputtering

had completely vanished after 42 days (Fig. 3e, f). Similar results were obtained already after 24 h of immersion, showing that this thin X-ray amorphous layer rapidly dissolves. This is in accordance to Refs. [31–33] where it was shown that crystalline calcium phosphate coatings dissolve slower than amorphous ones. The elemental composition of the coatings was determined by EDX (Fig. 3b, d and f). For the coatings deposited at 290 W, the Ca/P ratio decreased from 1.67 to 1.75 (before immersion) to 1.56 to 1.65 (after immersion). Note that the theoretical value for hydroxyapatite is 1.67. The decrease in the Ca/P ratio after immersion (290 W sample) may be due to the fact that amorphous calcium oxide (CaO) was also formed by the sputtering process (as reported in Ref. [34]) and preferentially dissolved during the immersion.

4 Conclusions

The release of nickel was considerable reduced by rf-magnetron sputtering of calcium phosphate on NiTi. No significant difference in the nickel release rate was found between pure water and aqueous saline solution when a power of 290 W was applied to deposit the coating

(thickness 0.6 μm). The average nickel release rate from the samples with this calcium phosphate coating was reduced by a factor of 7–10 in comparison to uncoated ones. No influence of the solution composition (water or 0.9% NaCl) on the nickel release rate was found. A thin amorphous coating that was deposited at 30 W was not suitable to constrain the release of nickel because it quickly disappeared from the surface of NiTi, either by dissolution or by delamination. It is concluded that a thicker and more crystalline coating is necessary to efficiently reduce the nickel release rate. In Ref. [18] it was shown that a nickel allergy can be triggered if the release of nickel exceeds a threshold of 0.5 $\mu g\ cm^{-2}\ week^{-1}$. Although the total amount of released nickel is far below this value even for pure NiTi, it is probably beneficial if the local concentration of nickel in the vicinity of surgical implants is decreased by a thin calcium phosphate coating.

Acknowledgements The authors thank Mr S. Boukercha, Mrs K. Brauner and Mrs V. Hiltenkamp for experimental assistance with the SEM experiments and with the nickel analyses.

References

1. Yahia L. Shape memory implants. Berlin: Springer; 2000.
2. Brantley WA, Eliades T. Orthodontic materials: scientific and clinical aspects. Stuttgart: Thieme; 2001. p. 310.
3. Zhao H, van Humbeeck J, de Scheerder I. Surface conditioning of nickel–titanium alloy stents for improving biocompatibility. Surf Eng. 2001;17:451–8.
4. Bansiddhi A, Sargeant TD, Stupp SI, Dunand DC. Porous NiTi for bone implants: a review. Acta Biomater. 2008;4:773–82.
5. Barouk LS. Osteotomies of the great toe. J Foot Surg. 1992;31:388–99.
6. Krone L, Mentz J, Bram M, Buchkremer HP, Stöver D, Wagner M, et al. The potential of powder metallurgy for the fabrication of biomaterials on the basis of nickel–titanium: a case study with a staple showing shape memory behaviour. Adv Eng Mater. 2005;7:613–9.
7. Agarwal P, Srivastava S, Srivastava MM, Prakash S, Ramanamurthy M, Shrivastav R, et al. Studies on leaching of Cr and Ni from stainless steel utensils in certain acids and in some Indian drinks. Sci Total Environ. 1997;199:271–5.
8. Mas A, Holt D, Webb M. The acute toxicity and teratogenicity of nickel in pregnant rats. Toxicology. 1985;35:47–57.
9. Wever DJ, Veldhuizen AG, Sanders MM, Schakenraad JM, van Horn JR. Cytotoxic, allergic and genotoxic activity of a nickel–titanium alloy. Biomaterials. 1997;18:1115–20.
10. Arndt MAB, Scully TAJ, Bourauel C. Nickel ion release from orthodontic NiTi wires under simulation of realistic in situ conditions. J Mater Sci. 2005;40:3659–67.
11. Shabalovskaya S, Anderegg J, van Humbeeck J. Critical overview of Nitinol surfaces and their modifications for medical applications. Acta Biomater. 2008;4:447–67.
12. Peitsch T, Klocke A, Kahl-Nieke B, Prymak O, Epple M. The release of nickel from orthodontic NiTi wires is strongly increased by dynamic mechanical loading but not constrained by surface nitridation. J Biomed Mater Res. 2007;82A:731–9.
13. Flyvholm MA, Nielsen GD, Andersen A. Nickel content of food and estimation of dietary-intake. Z Lebensmittelunters Forsch. 1984;179:427–37.
14. Herting G, Wallinder IO, Leygraf C. Factors that influence the release of metals from stainless steels exposed to physiological media. Corrosion Sci. 2006;48:2120–32.
15. Reclaru L, Lüthy H, Ziegenhagen R, Eschler PY, Blatter A. Anisotropy of nickel release and corrosion in austenitic stainless steels. Acta Biomater. 2008;4:680–5.
16. Yeung KWK, Chan RYL, Lam KO, Wu SL, Liu XM, Chung CY, et al. In vitro and in vivo characterization of novel plasma treated nickel titanium shape memory alloy for orthopedic implantation. Surf Coat Technol. 2007;202:1247–51.
17. Liu XM, Wu SL, Chu PK, Chung CY, Chu CL, Chan YL, et al. In vitro corrosion behavior of TiN layer produced on orthopedic nickel–titanium shape memory alloy by nitrogen plasma immersion ion implantation using different frequencies. Surf Coat Technol. 2008;202:2463–6.
18. Milosev I, Kosec T. Metal ion release and surface composition of the Cu-18Ni-20Zn nickel–silver during 30 days immersion in artificial sweat. Appl Surf Sci. 2007;254:644–52.
19. Colin S, Jolibois H, Chambaudet A, Tireford M. Corrosion stability of nickel in Ni alloys in synthetic sweat. Int Biodeterior Biodegrad. 1994;34:131–41.
20. Chan YL, Wu SL, Liu XM, Chu PK, Yeung KWK, Lu WW, et al. Mechanical properties, bioactivity and corrosion resistance of oxygen and sodium plasma treated nickel titanium shape memory alloy. Surf Coat Technol. 2007;202:1308–12.
21. Poon RWY, Yeung KWK, Liu XY, Chu PK, Chung CY, Lu WW, et al. Carbon plasma immersion ion implantation of nickel–titanium shape memory alloys. Biomaterials. 2005;26:2265–72.
22. Wever DJ, Veldhuizen AG, de Vries J, Busscher HJ, Uges DRA, van Horn JR. Electrochemical and surface characterization of a nickel–titanium alloy. Biomaterials. 1998;19:761–9.
23. Dorozhkin SV, Epple M. Biological and medical significance of calcium phosphates. Angew Chem Int Ed. 2002;41:3130–46.
24. Jiang HC, Rong LJ. Effect of hydroxyapatite coating on nickel release of the porous NiTi shape memory alloy fabricated by SHS method. Surf Coat Technol. 2006;201:1017–21.
25. Köller M, Esenwein SA, Bogdanski D, Prymak O, Epple M, Muhr G. Regulation of leukocyte adhesion molecules by leukocyte/biomaterial-conditioned media: a study with calcium phosphate-coated and non-coated NiTi-shape memory alloys. Matwiss u Werkstofftech. 2006;37:558–62.
26. Prymak O, Bogdanski D, Esenwein SA, Köller M, Epple M. NiTi shape memory alloys coated with calcium phosphate by plasma-spraying. Chemical and biological properties. Mat-wiss u Werkstofftech. 2004;35:346–51.
27. Choi J, Bogdanski D, Köller M, Esenwein SA, Müller D, Muhr G, et al. Calcium phosphate coating on nickel–titanium shape memory alloys. Coating procedure and adherence of leukocytes and platelets. Biomaterials. 2003;24:3689–96.
28. Xu S, Long J, Sim L, Diong CH, Ostrikov K. RF plasma sputtering deposition of hydroxyapatite bioceramics: synthesis, performance, and biocompatibility. Plasma Proc Polym. 2005;2:373–90.
29. Long J, Sim L, Xu S, Ostrikov K. Reactive plasma-aided RF sputtering deposition of hydroxyapatite bio-implant coatings. Chem Vap Deposition. 2007;13:299–306.
30. Pichugin VF, Surmenev RA, Shesterikov EV, Ryabtseva MA, Eshenko EV, Tverdokhlebov SI, et al. The preparation of calcium phosphate coatings on titanium and nickel–titanium by rf-magnetron-sputtered deposition: composition, structure and micromechanical properties. Surf Coat Technol. 2008;202:3913–20.
31. Ong JL, Lucas LC, Lacefield WR, Rigney ED. Structure, solubility and bond strength of thin calcium phosphate coatings

produced by ion beam sputter deposition. Biomaterials. 1992;13:249–54.
32. Cleries L, Fernandez-Pradas JM, Morenza JL. Bone growth on and resorption of calcium phosphate coatings obtained by pulsed laser deposition. J Biomed Mater Res. 2000;49:43–52.
33. Gledhill HC, Turner IG, Doyle C. In vitro dissolution behaviour of two morphologically different thermally sprayed hydroxyapatite coatings. Biomaterials. 2001;22:695–700.
34. Sivaram S. Chemical vapor deposition: thermal and plasma deposition of electronic materials. New York: International Thompson Publishing Inc.; 2000.